

## Effective ANN interactions in light hypernuclei

Yasuo Yamamoto

Physics Section, Tsuru University, Tsuru, Yamanashi 402, Japan

(Received 8 June 1987)

Microscopic cluster models for  $A=3-9$  are calculated with use of Gaussian-type  $\Lambda$ N and ANN interactions. Use of the strongly repulsive ANN interactions makes it possible to reproduce systematically  $\Lambda$  binding energies of  $s$ -shell and light  $p$ -shell hypernuclei. In the case of  ${}^{16}_{\Lambda}\text{O}$  the  $\Lambda$ N + ANN interaction produces results similar to a density-dependent  $\Lambda$ N interaction.

Calculated ground state  $\Lambda$  separation energies  $B_{\Lambda}$  in hypernuclei comprise a fundamental quantity which embodies aspects of both hypernuclear structure and the underlying  $\Lambda$ N interaction. Microscopic cluster models have been successfully applied by Motoba *et al.* to the systematic study of light  $p$ -shell hypernuclei.<sup>1</sup> Their cluster model approach is very useful to investigate the relation between  $B_{\Lambda}$  and  $\Lambda$ N interactions on realistic grounds, because relative motions among  $\Lambda$  and nuclear clusters are accurately taken into account. On this point there still remains quantitative problems; for instance, the calculated value of  $B_{\Lambda}$  for  ${}^9_{\Lambda}\text{Be}$  ( $\alpha+\alpha+\Lambda$ ) is overbound by 0.8 MeV, though their  $\Lambda$ N interaction is adjusted so as to reproduce the  $B_{\Lambda}$  value of  ${}^5_{\Lambda}\text{He}$  ( $\alpha+\Lambda$ ). This overbinding problem should not be overlooked, and neither should the famous  $s$ -shell one, since  ${}^9_{\Lambda}\text{Be}$  is of simple and typical cluster structure.

Bodmer *et al.* have showed that the  $B_{\Lambda}$  values of  $s$ -shell hypernuclei and  ${}^9_{\Lambda}\text{Be}$  can be consistently reproduced using not only the two-body  $\Lambda$ N interaction but also the Wigner-type repulsive three-body ANN interaction.<sup>2</sup> In our previous works<sup>3</sup> we represented the density-dependent  $\Lambda$ N interaction, designated YNG, on the basis of the  $G$ -matrix calculation with the Nijmegen model D interaction<sup>4</sup> and pointed out the important roles of the density dependence for  $B_{\Lambda}$  values and energy spectra. However, the notion of density dependence may be questionable for light clustering systems and is also computationally impracticable. Bodmer *et al.* consider that their phenomenological ANN interaction is due to some dispersive effect in the nuclear medium similar in origin to the density dependence.<sup>5</sup> On the other hand, Takeuchi and Shimizu have suggested that the large repulsive ANN interaction originates from the effect of quark antisymmetrization in hypernuclear systems.<sup>6</sup> In this situation it is very important to study the effect of repulsive ANN interactions in hypernuclei in detail, though its origin is not yet settled. In this paper we perform cluster model calculations for  $A=3-9$  hypernuclei with the explicit use of ANN interactions which are phenomenologically represented by Gaussian forms, and also discuss the similarity to the density-dependent effect in the case of  ${}^{16}_{\Lambda}\text{O}$ .

In the same manner as Ref. 1, we adopt microscopic

cluster models for  $s$ -shell and light  $p$ -shell hypernuclei.  ${}^5_{\Lambda}\text{He}$  and  ${}^4_{\Lambda}\text{He}({}^4_{\Lambda}\text{H})$  are described by  $\alpha$ - $\Lambda$  and  ${}^3\text{He}({}^3\text{H})$ - $\Lambda$  cluster wave functions, respectively, in which center of mass wave functions are extracted. Nuclear clusters are represented by harmonic oscillator wave functions (HOWF's) with size parameter  $b_N$ . Relative motions between  $\Lambda$  and clusters are treated by the generator coordinate method (GCM). The  $p$ -shell hypernuclei are described by the  $\alpha+x+\Lambda$  model ( $x=n$ ,  ${}^2\text{H}$ ,  ${}^3\text{H}$ ,  ${}^3\text{He}$ , or  $\alpha$ ). The GCM wave function of a hypernucleus ( $\alpha+x+\Lambda$ ) with total angular momentum  $J$  is symbolically expressed as

$$\Psi_J = \sum_c \sum_{dD} f_c(d, D) | [\Phi_l(d)\varphi_{\lambda}(D)]_L [S_x S_{\Lambda}]_S; J \rangle, \quad (1)$$

where  $d$  and  $D$  denote the generator coordinates which specify the  $\alpha$ - $x$  and  $(\alpha x)$ - $\Lambda$  distances, respectively, and  $\Phi_l(d)$  and  $\varphi_{\lambda}(D)$  and the corresponding basis wave functions with angular momenta  $l$  and  $\lambda$ . Spins are denoted by  $S_x$ ,  $S_{\Lambda}$ , and totally  $S$ ; then, an angular momentum channel is given by  $c = \{l, \lambda, L, S\}$ . From (1) we can obtain the channel-coupled Hill-Wheeler equation for the weight function  $f_c(d, D)$ . Interactions between  $\alpha$  and  $x$  are given by the orthogonality condition model<sup>7</sup> (OCM), which can nicely reproduce the  $\alpha+x$  two-cluster systems. Coulomb interactions between  $\alpha$  and  $x$  are also included. The expressions of GCM kernels and the interaction parameters of OCM are in Ref. 1. Furthermore, kernels for ANN interactions can be constructed straightforwardly owing to the Gaussian forms.

For the two-body  $\Lambda$ N part we use the  $G$ -matrix interaction calculated in nuclear matter at  $k_F=0.9 \text{ fm}^{-1}$  with the Nijmegen interaction. The potential form of this effective interaction is expressed in a superposition of Gaussian functions in the same way as Ref. 3:

$$V_{\Lambda N} = \sum_i v_i \exp[-(r/\beta_i)^2]. \quad (2)$$

Here the long range part is determined so as to simulate the spacially represented  $G$  matrices and the short range one is adjusted to reproduce the partial wave contribution of the  $\Lambda$  potential energy in nuclear matter. The ANN part of a Wigner type is phenomenologically represented by one range Gaussian form:

TABLE I. Interaction parameters of  $V_{\text{AN}}$ .  ${}^1E$ ,  ${}^3E$ ,  ${}^1O$ , and  ${}^3O$  denote singlet-even, triplet-even, singlet-odd, and triplet-odd states, respectively.

		No. 1		
$\beta_i$ (fm)		2.5	0.9	0.5
$v_i$ (MeV)	${}^1E$	-10.03	-297.7	1146
	${}^3E$	-9.895	-204.4	854.9
	${}^1O$	-5.494	-88.79	101.4
	${}^3O$	-8.384	-80.47	922.7
		No. 2		
$\beta_i$ (fm)		1.2	0.6	
$v_i$ (MeV)	${}^1E$	-58.25	45.75	
	${}^3E$	-51.42	100.8	
	${}^1O$	-27.06	-274.7	
	${}^3O$	-36.71	160.1	

$$V_{\text{ANN}} = w \exp[-(r_{1\Lambda}^2 + r_{2\Lambda}^2)/\beta_w^2], \quad (3)$$

where  $r_{i\Lambda} = r_\Lambda - r_i$  is a relative coordinate between  $\Lambda$  and N. The parameters  $w$  and  $\beta_w$  are adjusted so as to reproduce the  $B_\Lambda$  values of  ${}^5_\Lambda\text{He}$ ,  ${}^4_\Lambda\text{He}({}^4_\Lambda\text{H})$ ,  ${}^4_\Lambda\text{He}^*({}^4_\Lambda\text{H}^*)$ , and  ${}^9_\Lambda\text{Be}$ , where  ${}^4_\Lambda\text{He}^*({}^4_\Lambda\text{H}^*)$  indicates excited  $1^+$  states. Size parameters  $b_N$  are taken as 1.358 and 1.5 fm for  $\alpha$  and  ${}^3\text{He}({}^3\text{H})$  clusters, respectively. As the experimental  $B_\Lambda$  values of  ${}^4_\Lambda\text{He}({}^4_\Lambda\text{H})$  and  ${}^4_\Lambda\text{He}^*({}^4_\Lambda\text{H}^*)$ , we use 2.22 and 1.12 MeV, respectively, which should be obtained without charge symmetry breaking interactions. According to the choice of  $V_{\text{ANN}}$  the innermost-range part of  $V_{\text{AN}}$  is readjusted. Additionally, the relative strength of singlet-even and triplet-even state ones is also corrected, because that of the Nijmegen interaction is inadequate to reproduce the relative energy between  $0^+$  and  $1^+$  states of  ${}^4_\Lambda\text{He}({}^4_\Lambda\text{H})$ .<sup>8</sup>

Our interaction parameters are tabulated in Tables I and II. Here we give the two versions, Nos. 1 and 2, the AN parts of which are of three and two range Gaussian forms, respectively. The former is essentially the same as that in Ref. 3 and characterized by the strong short range repulsion. The latter is the *mild* version in which the intermediate range attraction and the short range repulsion are fairly canceled. This is similar to the effective AN interaction of Dover and Gal, which was obtained from the  $G$ -matrix calculation based on the simple separation method with the Nijmegen interaction.<sup>9</sup> These two versions have been designed to investigate how results are affected by the potential form, especially the short range repulsion.

TABLE II. Interaction parameters of  $V_{\text{ANN}}$ .

No.	$\beta_w$ (fm)	$w$ (MeV)
1	0.90	150.0
2	0.74	430.0

TABLE III. Calculated values of  $B_\Lambda$  (in MeV). The experimental values of  $A=4$  hypernuclei are the charge symmetric parts. Size parameters of nuclear clusters are  $b_N=1.358$  fm, except the  $A=4$  case ( $b_N=1.5$  fm).

	No. 1	No. 2	ORG	Expt.
${}^3_\Lambda\text{H}$	0.3	0.26	unbound	$0.13 \pm 0.05$
${}^4_\Lambda\text{He}({}^4_\Lambda\text{H})$	2.22	2.22	0.62	* $2.22 \pm 0.04$
${}^4_\Lambda\text{He}^*({}^4_\Lambda\text{H}^*)$	1.11	1.11	0.00	$1.12 \pm 0.06$
${}^5_\Lambda\text{He}$	3.12	3.12	3.11	$3.12 \pm 0.02$
${}^6_\Lambda\text{He}$	4.09	4.20	3.89	$4.25 \pm 0.10$
${}^7_\Lambda\text{Li}$	5.66	5.80	5.53	$5.58 \pm 0.03$
${}^8_\Lambda\text{Li}$	6.59	6.73	6.72	$6.80 \pm 0.03$
${}^8_\Lambda\text{Be}$	6.56	6.69	6.61	$6.84 \pm 0.05$
${}^9_\Lambda\text{Be}$	6.73	6.71	7.44	$6.71 \pm 0.04$

Now calculations are performed with our AN + ANN interactions and also the simple one-range-Gaussian (ORG) AN interaction used in Ref. 1. The ORG is adjusted so as to reproduce the  $B_\Lambda$  value of  ${}^5_\Lambda\text{He}$  for  $b_N=1.358$  fm. In the case of  ${}^4_\Lambda\text{He}({}^4_\Lambda\text{H})$ , however, the ORG gives only  $B_\Lambda=0.62$  MeV for  $b_N=1.5$  fm. As another check of effective interactions, we evaluate simply the  $B_\Lambda$  value of  ${}^3_\Lambda\text{H}$  described by the  $p+n+\Lambda$  three-body model. The treatment is in the same way as the  $\alpha+x+\Lambda$  model, where the  $pn$  interaction is central and reproduces the deuteron binding energy. Our No. 1 and No. 2 interactions give  $B_\Lambda=0.32$  and 0.26 MeV, respectively, for the observed value 0.13 MeV; the ORG gives no bound state. Thus our AN + ANN interactions are fairly free from the  $s$ -shell overbinding problem, differently from ORG.

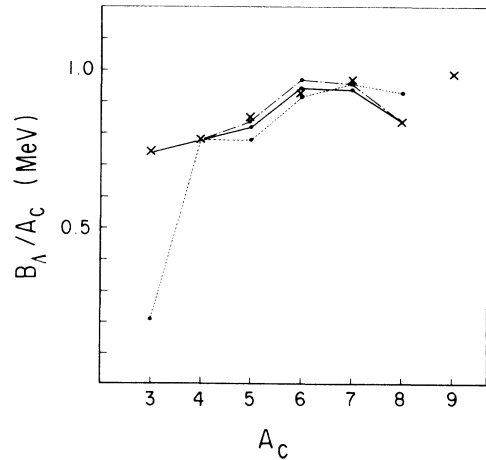


FIG. 1. Values of  $B_\Lambda/A_c$  calculated with use of No. 1, No. 2, and ORG interactions, which are connected by solid, dotted-dashed, and dotted lines, respectively. The  $A_c=7$  ones are for  ${}^8_\Lambda\text{Li}$ . The experimental ones are indicated by crosses.

TABLE IV. Root-mean-square estimates  $(\langle R^2 \rangle_\Lambda)^{1/2}$  and  $(\langle r^2 \rangle_{\alpha-x})^{1/2}$  of  $\Lambda$ -( $\alpha x$ ) and  $\alpha$ - $x$ .

	$(\langle R^2 \rangle_\Lambda)$ (fm)			$(\langle r^2 \rangle_{\alpha-x})$ (fm)		
	No. 1	No. 2	ORG	No. 1	No. 2	ORG
${}^6_\Lambda\text{He}$	2.93	2.79	2.54	3.76	3.68	3.48
${}^7_\Lambda\text{Li}$	2.82	2.69	2.42	3.43	3.37	3.13
${}^8_\Lambda\text{Li}$	2.75	2.63	2.37	3.46	3.42	3.20
${}^8_\Lambda\text{Be}$	2.76	2.64	2.38	3.49	3.45	3.23
${}^9_\Lambda\text{Be}$	2.78	2.69	2.39	3.72	3.68	3.44

Calculated  $B_\Lambda$  values are given in Table III. In these calculations GCM mesh points and angular momentum channels are taken in much the same way as Ref. 1. Our  $\Lambda N + \Lambda NN$  interactions turn out to reproduce the experimental values more systematically than the ORG: The  $\chi^2$  values for  $A > 5$  hypernuclei are 4.5, 3.4, and 19 in the cases of No. 1, No. 2, and ORG, respectively. The No. 1 and No. 2 interactions bring about no essential difference. The reason why the  $B_\Lambda$  values of  ${}^8_\Lambda\text{Li}$  are larger than those of  ${}^8_\Lambda\text{Be}$ , contrary to the observed ones, is considered to be because the charge symmetry breaking interaction is not taken into account. In order to see our result more obviously, we illustrate the values of  $B_\Lambda/A_c$  in Fig. 1, where  $A_c$  denotes a mass number of the nuclear core. The observed value of  $B_\Lambda/A_c$  for  $A_c=8$  is found to be especially small. This behavior cannot be reproduced by the ORG, which is the above-mentioned  ${}^9_\Lambda\text{Be}$  overbinding problem. It should be noted that this point is remarkably improved by the ANN interactions. Table IV shows root-mean-square estimates  $(\langle R^2 \rangle_\Lambda)^{1/2}$  and  $(\langle r^2 \rangle_{\alpha-x})^{1/2}$  for the  $\alpha+x+\Lambda$  systems, of the  $\Lambda$ -( $\alpha x$ ) and the  $\alpha$ - $x$  distance, respectively. Generally, our  $\Lambda N + \Lambda NN$  interactions give larger values than the ORG. The  $(\langle r^2 \rangle_{\alpha-x})^{1/2}$  values for  ${}^9_\Lambda\text{Be}$  are near the value 3.82 fm in Ref. 2. In Fig. 2 the calculated energy spectra of  ${}^9_\Lambda\text{Be}$  are shown in the cases of the No. 1 interaction and the ORG. Both results are quite similar to each other: The ANN interaction has no distinctive effect for energy spectra.

Let us compare our  $\Lambda NN$  interactions with that of Ref. 2. In their approach the original interaction  $V_{\Lambda NN}$  and the effective one  $\tilde{V}_{\Lambda NN}$  are used properly in the variational calculations for  $A < 5$  hypernuclei and the folding model one for  ${}^9_\Lambda\text{Be}$ , where  $\tilde{V}_{\Lambda NN}$  is obtained from  $V_{\Lambda NN}$  by multiplying the correlation factors. Our  $\Lambda NN$  interactions correspond rather to  $\tilde{V}_{\Lambda NN}$ , not  $V_{\Lambda NN}$ , though no explicit form of  $\tilde{V}_{\Lambda NN}$  is in Ref. 2 and we cannot compare the two directly. It is possible, however, to see the partial contributions of the  $\Lambda NN$  interactions to the  $\Lambda$  potential energies of  ${}^5_\Lambda\text{He}$  in both cases. It is reported in Ref. 2 that the variational and effective interaction calculations agree well for  ${}^5_\Lambda\text{He}$ , and the contributions of the  $\Lambda N$  and  $\Lambda NN$  parts are  $-11.28$  and  $2.35$  MeV, respectively, for the interaction parameters to reproduce the  $B_\Lambda$  value of  ${}^9_\Lambda\text{Be}$ . The corresponding values obtained from our No. 1 (No. 2) interaction are  $-11.69$  ( $-13.19$ ) and  $2.42$  ( $3.36$ ) MeV, respectively. The No. 1 interaction is noted to be fairly similar to theirs.

Finally, we discuss the relation between the present interaction and the density-dependent YNG interaction.<sup>3</sup> In Ref. 3 the shell model calculations for  $\Lambda$ -particle- $N$ -hole states of  ${}^{16}_\Lambda\text{O}$  were performed with YNG including the spin-orbit  $\Lambda N$  interaction and the antisymmetric one, where a  $\Lambda$  single particle state was represented by several terms of HOWF's. An average density approximation for each  $\Lambda$  state was used in this calculation; it has been shown by Kohno that similar results can be obtained with a more accurate local density approximation.<sup>10</sup> Here we perform the same calculation using the No. 1 interaction. The  $\Lambda N + \Lambda NN$  interaction, parameters of which are adjusted using  $B_\Lambda$  values of light systems, has a tendency to result in overly large values of  $B_\Lambda$  in heavier ones, as is seen also in Ref. 2. So we multiply an enhancement factor 1.035 on the even state core parts of the  $\Lambda N$  interaction, while the  $\Lambda NN$  part is not changed. The value of this factor is chosen so as to reproduce the same value of  $B_\Lambda$  as YNG for the  ${}^{16}_\Lambda\text{O}$  ground configuration  $[(s_{1/2})_\Lambda(0p_{1/2})_{\bar{N}}^{-1}]_{1^-}$ . The  $B_\Lambda$  value changes by 2.0 MeV due to this factor. We proceed to calculate in much the same way as Ref. 3 for the ground configuration and the two recoilless  $0^+$  states treated as a mixture of two configurations  $[(p_{1/2})_\Lambda(0p_{1/2})_{\bar{N}}^{-1}]_{0^+}$  and  $[(p_{3/2})_\Lambda(0p_{3/2})_{\bar{N}}^{-1}]_{0^+}$  corre-

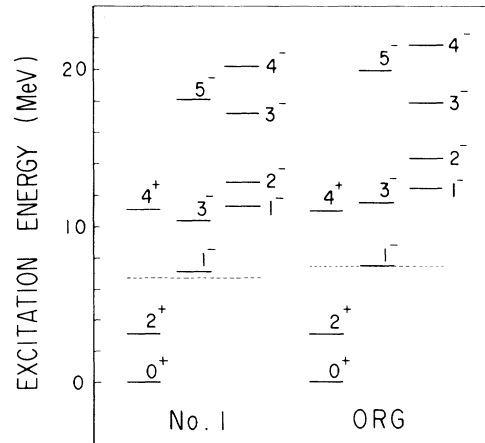


FIG. 2. Calculated energy spectra of  ${}^9_\Lambda\text{Be}$  with No. 1 and ORG interactions, where levels are assigned orbital angular momentum  $L$  instead of degenerate  $J=L+\frac{1}{2}$ . The dotted lines indicate  $\Lambda$  threshold energies.

TABLE V. Eigenenergies (in MeV) of  $\Lambda$ -particle-N-hole states of  ${}^{16}_\Lambda\text{O}$ . The YNG result is cited from Ref. 3.

Main component	No. 1	YNG	Expt.
$[(p_{3/2})_\Lambda(0p_{3/2})\bar{n}^{-1}]_{0+}$	3.43	3.47	3.5
$[(p_{1/2})_\Lambda(0p_{1/2})\bar{n}^{-1}]_{0+}$	-2.48	-2.58	-2.5
$[(s_{1/2})_\Lambda(0p_{1/2})\bar{n}^{-1}]_{1-}$	-12.1	-12.1	-13

sponding to the  $(K^-, \pi^-)$  reaction data.<sup>11</sup> It is straightforward to taken into account the  $\Lambda\text{NN}$  part in our framework. The calculated result is shown in Table V together with the YNG result in Ref. 3 and the experimental data. The  $\Lambda\text{N} + \Lambda\text{NN}$  interaction is found to lead to the quite similar result as the density-dependent one in this case. Here it should be noted that the  $\Lambda\text{NN}$  part of the former has been determined phenomenologically and the density dependence of the latter is based on the  $G$ -matrix calculation with the Nijmegen interaction. Thus it seems acceptable to consider that the two are

different expressions for the dispersive effect in nuclear medium.

To summarize, we have proposed use of the  $\Lambda\text{N} + \Lambda\text{NN}$  interactions with Gaussian forms to facilitate convenient application to microscopic cluster models. The two-body  $\Lambda\text{N}$  interactions are parametrized on the basis of the  $G$ -matrix calculation with the Nijmegen model D interaction. The three-body  $\Lambda\text{NN}$  interactions are phenomenologically determined so as to reproduce  $B_\Lambda$  values of some typical hypernuclei. Our effective interactions have been applied to the microscopic cluster models for  $A = 3-9$  hypernuclei. Owing to the  $\Lambda\text{NN}$  parts the observed  $B_\Lambda$  values can be reproduced systematically. In a heavier system such as  ${}^{16}_\Lambda\text{O}$  the  $\Lambda\text{N} + \Lambda\text{NN}$  interaction works in a way similar to the density-dependent  $\Lambda\text{N}$  interaction.

The author is very grateful to Professor H. Bando for helpful discussions on cluster model calculations. Numerical calculations were carried out at the INS Computer Center at the University of Tokyo.

- <sup>1</sup>T. Motoba, H. Bando, and K. Ikeda, *Prog. Theor. Phys.* **70**, 189 (1983); T. Motoba, H. Bando, K. Ikeda, and T. Yamada, *Prog. Theor. Phys. Suppl. No. 81*, 42 (1985).  
<sup>2</sup>A. R. Bodmer, Q. N. Usmani, and J. Carlson, *Phys. Rev. C* **29**, 684 (1984).  
<sup>3</sup>Y. Yamamoto and H. Bando, *Prog. Theor. Phys.* **73**, 905 (1985); *Prog. Theor. Phys. Suppl. No. 81*, 9 (1985).  
<sup>4</sup>M. M. Nagels, T. A. Rijken, and J. J. deSwart, *Phys. Rev. D* **12**, 744 (1975); **15**, 2547 (1977); **20**, 1633 (1979).  
<sup>5</sup>A. R. Bodmer and Q. N. Usmani, in *Proceedings of the International Symposium on Hypernuclear and Kaon Physics*,

- edited by R. E. Chrien [*Nucl. Phys.* **A450**, 257c (1986)].  
<sup>6</sup>S. Takeuchi and K. Shimizu, *Phys. Lett. B* **179**, 197 (1986).  
<sup>7</sup>S. Saito, *Prog. Theor. Phys.* **40**, 893 (1968); **41**, 705 (1969).  
<sup>8</sup>H. Bando, *Prog. Theor. Phys.* **66**, 1349 (1981).  
<sup>9</sup>C. B. Dover and A. Gal, in *Progress in Particle and Nuclear Physics*, edited by D. Wilkinson (Pergamon, Oxford, 1984), Vol. 12.  
<sup>10</sup>M. Kohno, *Prog. Theor. Phys.* **78**, 123 (1987).  
<sup>11</sup>W. Brückner *et al.*, *Phys. Lett.* **79B**, 157 (1978); A. Bouyssy, *ibid.* **84B**, 41 (1979); **91B**, 15 (1980).